

## Activation of Metallocenes for Olefin Polymerization As Monitored by IR Spectroscopy

Jan L. Eilertsen,<sup>\*†</sup> Jon A. Støvneng,<sup>‡</sup> Martin Ystenes,<sup>§</sup> and Erling Rytter<sup>†||</sup>

Department of Chemical Engineering, Department of Physics, and Department of Materials Science, Norwegian University of Science and Technology, N-7491 Trondheim, Norway, and Statoil Research Centre, N-7005 Trondheim, Norway

Received December 10, 2004

Binary mixtures of  $\text{Cp}_2\text{ZrMe}_2$ ,  $\text{Cp}_2\text{ZrCl}_2$ , dimethylaluminum chloride, trimethylaluminum, and methylaluminoxane (MAO), as well as  $\text{Cp}_2\text{ZrMe}_2$  with boron-based activators, have been studied by in situ IR spectroscopy (Cp = cyclopentadienyl, Me = methyl). The position of a strong band near  $800\text{ cm}^{-1}$ , corresponding to the out-of-plane vibration of the Cp hydrogen atoms, is sensitive to the bonding environment around Zr and can be used to monitor reactions and the formation of new products in these mixtures. Harmonic frequencies determined by density functional theory correlate well with experimental values and have been used to assist in the interpretation of the data. The frequency of the Cp out-of-plane vibration, ranging from  $797$  to  $832\text{ cm}^{-1}$  in our experiments, is found to increase with increasing electron density on the Cp ring and decreasing Zr–Cp distance. In the mixture of MAO and  $\text{Cp}_2\text{ZrMe}_2$ , a stable complex is rapidly formed at low Al/Zr ratios. A mechanism that may explain the need for a large MAO excess is proposed for the activation of metallocenes with MAO. The proposed mechanism involves the formation of dimers or oligomers of MAO cages that tend to dissipate the charge of the anion. This destabilization of the  $\text{Cp}_2\text{ZrMe}_2$ –MAO complex facilitates the formation of the catalytically active cation.

### Introduction

The oligomeric compound methylaluminoxane (MAO) is known as a highly efficient activator for metallocene catalysts of olefin polymerization.<sup>1,2</sup> Despite considerable effort to resolve its structure and determine how MAO takes part in the activation of the catalyst, these questions are still largely unanswered. The metallocene part of the catalyst system is far better understood, mainly, because of studies with well-defined boron activators.<sup>1</sup> Several intermediates in boron-activated systems have been identified by NMR spectroscopy or X-ray diffraction. By comparison of NMR shifts, several cationic Zr species have also been identified in the metallocene/MAO system.<sup>3,4</sup> Further evidence has been obtained by UV–vis spectroscopy, which is insensitive to the large

amount of MAO present under normal polymerization conditions.<sup>5</sup> IR and NMR spectroscopy respond differently to fast chemical exchange among multiple components because of their different characteristic time scales. In IR spectroscopy, the individual components are observed, while in the NMR spectrum, an average signal appears. Recently, new results on the structure of MAO have been obtained by in situ IR spectroscopy.<sup>6,7</sup> In particular, bridging methyl groups were identified as an essential part of the MAO structure and found to be crucial to the metallocene activation. The bridging methyl groups were not recognized in NMR studies.

\* To whom correspondence should be addressed. Fax: +47 73594080. E-mail: eilerts@chem.ntnu.no.

† Department of Chemical Engineering, Norwegian University of Science and Technology.

‡ Department of Physics, Norwegian University of Science and Technology.

§ Department of Materials Science, Norwegian University of Science and Technology.

|| Statoil Research Centre.

(1) Bochmann, M. *J. Chem. Soc., Dalton Trans.* **1996**, 255–270.

(2) Chen, E. Y.-X.; Marks, T. J. *Chem. Rev.* **2000**, *100*, 1391–1434.

(3) Babushkin, D. E.; Semikolenova, N. V.; Zakharov, V. A.; Talsi, E. *Macromol. Chem. Phys.* **2000**, *201*, 558–567.

(4) Tritto, I.; Donetti, R.; Sacchi, M. C.; Locatelli, P.; Zannoni, G. *Macromolecules* **1997**, *30*, 1247–1252.

(5) (a) Coevoet, D.; Cramail, H.; Deffieux, A. *Macromol. Chem. Phys.* **1998**, *199*, 1451–1457. (b) Pedetour, J.-N.; Radhakrishnan, K.; Cramail, H.; Deffieux, A. *Polym. Int.* **2002**, *51*, 973–977. (c) Pedetour, J.-N.; Radhakrishnan, K.; Cramail, H.; Deffieux, A. *J. Mol. Catal. A* **2002**, *185*, 119–125.

(6) Eilertsen, J. L.; Rytter, E.; Ystenes, M. *Vib. Spectrosc.* **2000**, *24*, 257–264.

(7) Ystenes, M.; Eilertsen, J. L.; Jianke, L.; Ott, M.; Rytter, E.; Støvneng, J. A. *J. Polym. Sci. A* **2000**, *38*, 3106–3127.

In the activation of metallocenes by MAO, the first step is the reversible formation of an adduct.<sup>3</sup> This is followed by the formation of the cationic species  $[(\text{Cp}_2\text{ZrMe})_2(\mu\text{-Me})]^+$ ,  $[\text{Cp}_2\text{Zr}(\mu\text{-Me})_2\text{AlMe}_2]^+$ , and  $[\text{Cp}_2\text{ZrMe}]^+$  (Cp = cyclopentadienyl, Me = methyl).<sup>3,4</sup> The unprotected cation  $[\text{Cp}_2\text{ZrMe}]^+$  is probably rare, and it has been proposed that the MAO anion coordinates through an unsymmetrical methyl bridge.<sup>3</sup> Trimethylaluminum (TMA) constitutes a significant part of commercial MAO solutions, but its full role in the activation is not clear.<sup>2,8</sup> TMA is able to monomethylate the metallocene, and then it reacts to form the  $[\text{Cp}_2\text{Zr}(\mu\text{-Me})_2\text{AlMe}_2]^+$  cation.<sup>4,5</sup>

In the present IR study, we investigated binary mixtures of  $\text{Cp}_2\text{ZrMe}_2$ ,  $\text{Cp}_2\text{ZrCl}_2$ , TMA, DMAC (dimethylaluminum chloride), and MAO, as well as mixtures of  $\text{Cp}_2\text{ZrMe}_2$  and boron-based activators. All reactions were studied in situ using a custom-built liquid flow cell constructed to meet the challenges of material inertness and sample handling posed by these reactive systems. The IR spectra of known and anticipated metallocene species were also investigated by density functional theory (DFT), focusing on the band corresponding to the out-of-plane vibration of the hydrogen atoms on the Cp ring, at around  $800\text{ cm}^{-1}$ . The position of this band is sensitive to changes in the bonding environment around the zirconium atom, and the correlation between observed band position and calculated structural parameters was investigated.

The metallocene/MAO systems, in which stable intermediates are observed at unexpectedly low Al/Zr ratios, are particularly interesting.<sup>9,10</sup> Possible structural candidates for these intermediates are discussed, as well as a mechanism to explain the need for a large MAO excess for the reaction.

## Experimental Section

**General.** All operations were carried out under a dry nitrogen or argon atmosphere (99.999%) using standard Schlenk techniques. Solids were handled in a glovebox. Solutions were transferred and metered with lubricant-free disposable syringes or gastight microsyringes. The IR spectra were recorded on a Bruker IFS66v spectrometer using a custom-built liquid flow cell.<sup>11</sup> The cell and the attached glass equipment make a closed loop consisting of a glass mixing tank (20 mL), a micropump to circulate the liquid, and the IR cell. The circulation ensures rapid mixing and constant sampling of the studied solution. Uniform mixing is achieved within 1–2 min after reactant addition. The entire sample passes through the loop during this time. A flow split leads about 10% of the flow between the windows. Silicon and germanium windows were used because MAO reacts with halide salts.<sup>12</sup> The spectra were recorded with a nominal resolution of  $2\text{ cm}^{-1}$  and zero-filled to  $0.5\text{ cm}^{-1}$ .

To obtain the spectra of the solute, the solvent spectrum was digitally removed using a spectrum of the pure solvent. The regions around  $740$  and  $690\text{ cm}^{-1}$  are obscured because of the strong bands for toluene.

The phase separation observed in the concentrated MAO/metallocene systems induces fluctuations in the intensity of the IR spectra.<sup>13</sup> A similar phase separation is observed in the  $\text{C}(\text{C}_6\text{F}_5)_3\text{B}(\text{C}_6\text{F}_5)_4/\text{Cp}_2\text{ZrMe}_2$  system and is responsible for the observed double set of  $^1\text{H}$  NMR peaks.<sup>14</sup> The spectra were recorded over 2 min (300 scans) with a constant circulation of the sample solution to ensure that the spectra were representative for both phases. Still, this was not adequate to average all fluctuations. The spectra of the MAO/metallocene system were therefore scaled to equal intensity at  $790\text{ cm}^{-1}$  for the purpose of observing relative changes in the IR bands. Studies of more dilute solutions were attempted to avoid phase separation, but a reliable analysis was, in this case, prevented by a low signal-to-noise ratio.

**Materials.** Trimethylaluminum (TMA) and dimethylaluminum chloride (DMAC) were purchased from Aldrich and used without further purification. The absence of air contamination products in MAO, TMA, and DMAC was verified by the absence of methoxy IR bands around  $990\text{ cm}^{-1}$ . Toluene, benzene, and tetrahydrofuran (THF) were refluxed over sodium/benzophenone and distilled under nitrogen before use. Pentane was dried with molecular sieves (3 Å). The MAO solution (Albemarle, 10 wt % in toluene) was solidified at room temperature under reduced pressure.  $\text{Cp}_2\text{ZrMe}_2$  (Strem Chemicals),  $\text{Cp}_2\text{ZrCl}_2$  (Boulder Scientific), tris(pentafluorophenyl)boron (Strem Chemicals), and trityl tetra(pentafluorophenyl)boron (Albemarle) were used as received.

**Preparations.** TMA-depleted MAO was prepared by removing the TMA and solvent from a commercial MAO solution by reduced pressure (to about 0.07 mbar) at room temperature. The solid MAO was redissolved in toluene, and the procedure was repeated to further reduce the amount of TMA. The solid was evacuated at less than 0.1 mbar for at least 2 h.  $\text{Cp}_2\text{ZrMeCl}$  was prepared from equimolar amounts of  $\text{Cp}_2\text{ZrCl}_2$  and  $\text{Cp}_2\text{ZrMe}_2$ .<sup>15</sup> The reaction took place over 2–3 weeks in benzene at room temperature.  $^1\text{H}$  NMR ( $d^8$  toluene):  $\delta$  0.45, Me; 5.78, Cp. IR:  $809\text{ cm}^{-1}$ .  $\text{Cp}_2\text{ZrMe}(\mu\text{-Me})\text{B}(\text{C}_6\text{F}_5)_3$  was prepared by mixing equimolar amounts of solid  $\text{Cp}_2\text{ZrMe}_2$  and  $\text{B}(\text{C}_6\text{F}_5)_3$ .<sup>16</sup> Benzene was added at  $-65\text{ }^\circ\text{C}$ , and the mixture was slowly heated and stirred for 2 h. Dry pentane was added, and the precipitate was filtered and washed three times with pentane.  $^1\text{H}$  NMR ( $d^8$  toluene):  $\delta$  0.26, 0.11, Me; 5.45, Cp. IR:  $825\text{ cm}^{-1}$ .  $(\text{Cp}_2\text{ZrMe})_2(\mu\text{-O})$  was prepared via the reaction of  $\text{Cp}_2\text{ZrMe}_2$  with water in THF.  $\text{Cp}_2\text{ZrMe}_2$  (0.13 g) was dissolved in 5 mL of tetrahydrofuran (THF), and the mixture was cooled to  $-35\text{ }^\circ\text{C}$ . Water (4.6 mg) dissolved in THF was added slowly, and the solution was slowly heated to room temperature. The solvent was removed by evaporation, and the solid residue was dissolved in toluene.  $^1\text{H}$  NMR ( $d^6$  benzene):  $\delta$  0.23, Me; 5.74, Cp. IR:  $797$  (Cp oop),  $740\text{ cm}^{-1}$  (Zr–O stretch). The NMR peaks are in agreement with literature data.<sup>17</sup> In addition to  $(\text{Cp}_2\text{ZrMe})_2(\mu\text{-O})$ , the product contained  $(\text{Cp}_2\text{ZrO})_3$ .  $^1\text{H}$  NMR:  $\delta$  6.21, Cp.<sup>18</sup>  $[(\text{Cp}_2\text{-}$

- (8) Imhoff, D. W.; Simeral, L. S.; Sangokoya, S. A.; Peel, J. H. *Organometallics* **1998**, *17*, 1941–1945.  
 (9) Eilertsen, J. L.; Støvneng, J. A.; Ystenes, M.; Rytter, E. In *Future Technology for Polyolefin and Olefin Polymerization Catalysis*; Terano, M., Shiono, T., Eds.; Technology and Educational Publishers: Tokyo, 2002; pp 111–116.  
 (10) Eilertsen, J. L.; Rytter, E.; Ystenes, M. In *Organometallic Catalysts and Olefin Polymerization*; Blom, R., Follestad, A., Rytter, E., Tilset, M., Ystenes, M., Eds.; Springer: Berlin, 2001; pp 86–96.  
 (11) Bache, Ø.; Ystenes, M. *Appl. Spectrosc.* **1993**, *48*, 985–993.  
 (12) Eilertsen, J. L. Doctoral Thesis, Norwegian University of Science and Technology, Trondheim, Norway, 2000, ISBN 82-7984-139-3.

- (13) Siedle, A. R.; Lamanna, W. M.; Newmark, R. A.; Schroepfer, J. N. *J. Mol. Catal. A* **1998**, *128*, 257–271.  
 (14) Talsi, E.; Eilertsen, J. L.; Ystenes, M.; Rytter, E. *J. Organomet. Chem.* **2003**, *677*, 10–14.  
 (15) Jordan, R. F. *J. Organomet. Chem.* **1985**, *294*, 321–326.  
 (16) Yang, X.; Stern, C. L.; Marks, T. J. *J. Am. Chem. Soc.* **1994**, *116*, 10015–10031.  
 (17) Marsella, J. A.; Folting, K.; Huffman, J. C.; Caulton, K. G. *J. Am. Chem. Soc.* **1981**, *103*, 5596–5598.  
 (18) Lukens, W. W.; Andersen, R. A. *Organometallics* **1995**, *14*, 3435–3439.

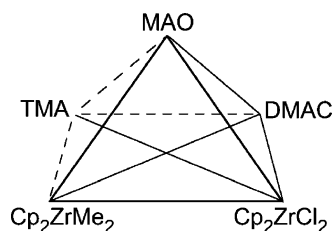


**Figure 1.** Overview of the aluminum-based systems studied. Dashed lines connect components whose mixture yielded no detectable new species. Solid lines indicate the formation of a new compound.

$(\text{Cp}_2\text{Zr}(\mu\text{-Me})^+)$  was prepared by mixing solutions of  $\text{C}(\text{C}_6\text{H}_5)_3\text{B}(\text{C}_6\text{F}_5)_4$  and  $\text{Cp}_2\text{ZrMe}_2$  directly in the in situ IR apparatus at room temperature.  $^1\text{H}$  NMR ( $d^6$  benzene):  $\delta$   $-0.09$ ,  $-1.22$ , Me;  $5.61$ , Cp. IR:  $818\text{ cm}^{-1}$ .  $[(\text{Cp}_2\text{Zr}(\mu\text{-Me})_2\text{AlMe}_2)^+]$  was prepared by adding excess TMA to the previous mixture and by adding TMA and a solution of  $\text{Cp}_2\text{ZrMe}_2$  to a solution of  $\text{C}(\text{C}_6\text{H}_5)_3\text{B}(\text{C}_6\text{F}_5)_4$ .  $^1\text{H}$  NMR ( $d^6$  benzene):  $\delta$   $-0.40$ ,  $-0.73$ , Me;  $5.44$ , Cp. IR:  $832\text{ cm}^{-1}$ .

**Computational Details.** All calculations are based on DFT. The programs used were ADF 2.3 (Scientific Computing and Modeling)<sup>19</sup> and Gaussian 03 (Gaussian Inc.)<sup>20</sup>. Different levels of computation were used to verify observed trends and correlation between the experiment and theory.

In ADF, the density functionals used were those of Vosko, Wilk, and Nusair (VWN)<sup>21</sup> for the local density part. Gradient corrections, based on the functionals proposed by Becke<sup>22</sup> for exchange and Perdew and Wang<sup>23</sup> for correlation (i.e., BPW91), were included self-consistently. We used a double- $\zeta$  Slater-type orbital basis set extended with a polarization function (DZP) for all atoms except Zr, for which a triple- $\zeta$  basis set (TZP) was used. The  $1s$ – $3d$  orbitals on Zr, the  $1s$ – $2p$  orbitals on Al and Cl, and the  $1s$  orbital on B, C, F, and O were treated within the frozen-core approximation.

In Gaussian, the following combinations of density functionals and basis sets were used: BPW91/3-21G\*\* ( $G_1$ ), B3LYP/3-21G\*\* ( $G_2$ ), and B3LYP/6-31+G(d,p) ( $G_3$ ). In the latter case, the effective core potential basis set, LANL2DZ, was used for Zr.

## Results

**Overview.** The various aluminum-based mixtures are depicted in Figure 1. Dashed lines indicate binary mixtures where no new products were detected by IR spectroscopy. Comparative studies were performed with the two well-

**Table 1.** Experimental and Calculated Band Positions ( $\text{cm}^{-1}$ ) of the Out-of-Plane Deformations of the C–H Bonds of the Cp Ring for Selected Zirconocenes and Complexes in Aromatic Solution

	compound	ADF <sup>b</sup>	$G_1^c$	$G_2^d$	$G_3^e$	exp
A <sup>a</sup>	$\text{Cp}_2\text{ZrMe}_2$	781	779	804	807	803
	$\text{Cp}_2\text{ZrMeCl}$	790	783	807	814	809
	$\text{Cp}_2\text{ZrCl}_2$	793	783	809	820	814
B <sup>a</sup>	$(\text{Cp}_2\text{ZrMe})_2(\mu\text{-O})$	777	780	797	803	797
	$[(\text{Cp}_2\text{ZrMe})_2(\mu\text{-Me})]^+$	794	799	822	821	818
	$\text{Cp}_2\text{ZrMe}(\mu\text{-Me})\text{BR}_3$	806	810	828	824	825
	$[\text{Cp}_2\text{Zr}(\mu\text{-Me})_2\text{AlMe}_2]^+$	810	807	839	834	832

<sup>a</sup> A: simple zirconocenes. B: complexes verified by  $^1\text{H}$  NMR. <sup>b</sup> BPW91/DZP, TZP. <sup>c</sup> BPW91/3-21G\*\*. <sup>d</sup> B3LYP/3-21G\*\*. <sup>e</sup> B3LYP/6-31+G(d,p), LANL2DZ. See Experimental Section for details.

characterized boron cocatalysts  $\text{B}(\text{C}_6\text{F}_5)_3$  and  $\text{C}(\text{C}_6\text{H}_5)_3\text{B}(\text{C}_6\text{F}_5)_4$  using both IR and NMR spectroscopy.

The  $\eta$ -5-cyclopentadienyl ligands of metallocenes have a relatively simple IR spectrum with a few strong bands.<sup>24</sup> The strongest band, caused by the out-of-plane deformations of the C–H bonds, is also the band most sensitive to changes in the coordination of Zr and therefore suitable for monitoring reactions. The positions of this band for simple zirconocenes (A) and four zirconocene complexes (B) are given in Table 1.

Theoretical IR spectra were calculated within the harmonic approximation. A single conformation with respect to the relative rotation of the Cp rings was used in the calculations. In general, this yields several close bands. The relative intensity of these bands varies somewhat with the chosen level of computation. Therefore, Lorentzians with widths between  $5$  ( $G_2$ )<sup>25</sup> and  $20\text{ cm}^{-1}$  (ADF)<sup>25</sup> were applied to form a single band, as observed in the experiments. The general appearance of the calculated spectra of  $\text{Cp}_2\text{ZrMe}_2$ ,  $\text{Cp}_2\text{ZrMeCl}$ , and  $\text{Cp}_2\text{ZrCl}_2$  is in good agreement with experiment. A comparison ( $G_3$ )<sup>25</sup> is shown for  $\text{Cp}_2\text{ZrMe}_2$  in Figure 2B. In Figure 2A, calculated ( $G_3$ ) and experimental Cp out-of-plane deformation bands at around  $800\text{ cm}^{-1}$  are shown for all three zirconocenes. Four additional zirconocene complexes have been verified with NMR spectroscopy. In Figure 3, calculated (ADF) and experimental band positions of the Cp out-of-plane deformations are compared for all seven verified complexes. The best linear fit is given by  $\nu(\text{exp}) = 1.005\nu(\text{ADF}) + 17$ . Corresponding lines obtained with Gaussian calculations are  $\nu(\text{exp}) = 0.829\nu(G_1) + 158$ ,  $\nu(\text{exp}) = 0.799\nu(G_2) + 163$ , and  $\nu(\text{exp}) = 1.145\nu(G_3) - 122$ .

In the present work, considerable effort has been directed toward gaining insight into how the position of the band resulting from the Cp out-of-plane deformation is influenced by changes in the steric and electronic environment of the zirconium atom. A multivariate analysis on the basis of the seven compounds listed in Table 1 showed that the band position correlates well with the calculated Mulliken charge on the Cp ring (in agreement with ref 24) as well as the distance between Zr and the center of the Cp ring. Other parameters, such as the charge on Zr and the Cp–Cp opening angle, showed poor correlation. The results suggest a shift

(19) ADF 2.3, *Scientific Computing and Modeling*; Chemistry Department, Vrije Universiteit: Amsterdam, The Netherlands, 1997.

(20) Frisch, M. J.; Trucks, G. W.; Schlegel, H. B.; Scuseria, G. E.; Robb, M. A.; Cheeseman, J. R.; Montgomery, J. A., Jr.; Vreven, T.; Kudin, K. N.; Burant, J. C.; Millam, J. M.; Iyengar, S. S.; Tomasi, J.; Barone, V.; Mennucci, B.; Cossi, M.; Scalmani, G.; Rega, N.; Petersson, G. A.; Nakatsuji, H.; Hada, M.; Ehara, M.; Toyota, K.; Fukuda, R.; Hasegawa, J.; Ishida, M.; Nakajima, T.; Honda, Y.; Kitao, O.; Nakai, H.; Klene, M.; Li, X.; Knox, J. E.; Hratchian, H. P.; Cross, J. B.; Bakken, V.; Adamo, C.; Jaramillo, J.; Gomperts, R.; Stratmann, R. E.; Yazyev, O.; Austin, A. J.; Cammi, R.; Pomelli, C.; Ochterski, J. W.; Ayala, P. Y.; Morokuma, K.; Voth, G. A.; Salvador, P.; Dannenberg, J. J.; Zakrzewski, V. G.; Dapprich, S.; Daniels, A. D.; Strain, M. C.; Farkas, O.; Malick, D. K.; Rabuck, A. D.; Raghavachari, K.; Foresman, J. B.; Ortiz, J. V.; Cui, Q.; Baboul, A. G.; Clifford, S.; Cioslowski, J.; Stefanov, B. B.; Liu, G.; Liashenko, A.; Piskorz, P.; Komaromi, I.; Martin, R. L.; Fox, D. J.; Keith, T.; Al-Laham, M. A.; Peng, C. Y.; Nanayakkara, A.; Challacombe, M.; Gill, P. M. W.; Johnson, B.; Chen, W.; Wong, M. W.; Gonzalez, C.; Pople, J. A. *Gaussian 03*, revision C.02; Gaussian, Inc.: Wallingford, CT, 2004.

(21) Vosko, S. H.; Wilk, L.; Nusair, M. *Can. J. Phys.* **1980**, *58*, 1200–1211.

(22) Becke, A. D. *Phys. Rev. A* **1988**, *38*, 3098–3100.

(23) Perdew, J. P.; Wang, Y. *Phys. Rev. B* **1992**, *45*, 13244–13249.

(24) Diana, E.; Rossetti, R.; Stanghellini, P. L.; Kettle, S. F. A. *Inorg. Chem.* **1997**, *36*, 382–391.

(25) See Experimental section or Table 1 for notation.

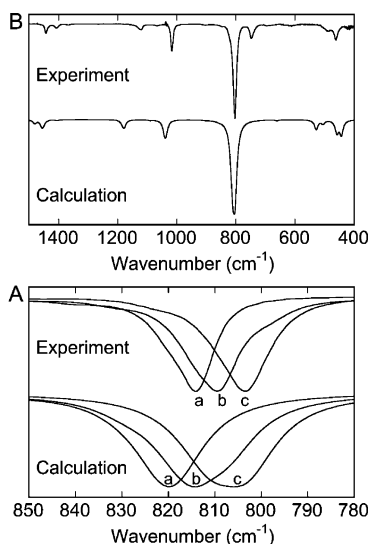


**Figure 2.** Comparison of calculated ( $G_3$ )<sup>25</sup> and measured IR spectra. Lorentzians with a width of  $7\text{ cm}^{-1}$  are used in the calculated spectra. A: (a)  $\text{Cp}_2\text{ZrCl}_2$ , (b)  $\text{Cp}_2\text{ZrMeCl}$ , and (c)  $\text{Cp}_2\text{ZrMe}_2$  in the  $780\text{--}850\text{ cm}^{-1}$  range. B:  $\text{Cp}_2\text{ZrMe}_2$  in the  $400\text{--}1500\text{ cm}^{-1}$  range. All spectra have been scaled to a common minimum value for the transmissivity. The band at  $750\text{ cm}^{-1}$  in the experimental spectrum of  $\text{Cp}_2\text{ZrMe}_2$  is probably the  $\text{Zr}\text{--}\text{O}$  stretch in  $(\text{Cp}_2\text{ZrMe})_2(\mu\text{-O})$ , which is caused by traces of oxygen impurities. The Cp out-of-plane vibration of  $(\text{Cp}_2\text{ZrMe})_2(\mu\text{-O})$  was found at  $797\text{ cm}^{-1}$  in a separate experiment.

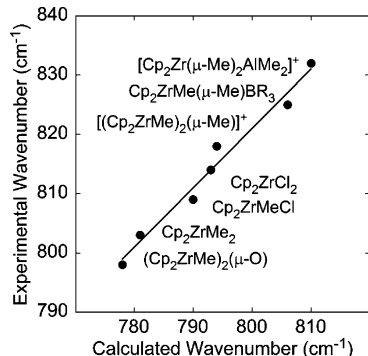


**Figure 3.** Comparison of measured and calculated (ADF)<sup>25</sup> frequencies for the out-of-plane C–H deformations of Cp. For the methyl-bridged complex with the boron cocatalyst,  $\text{CF}_3$  model ligands on B were used:  $\text{R}=\text{CF}_3$  (calculation),  $\text{C}_6\text{F}_5$  (experiment). We have verified, at the  $G_1$  and  $G_2$  levels,<sup>25</sup> that calculations with  $\text{R}=\text{C}_6\text{F}_5$  yield essentially identical band positions. Corresponding curves based on band positions calculated with Gaussian show a similar correlation, with the exception of level  $G_1$ . Deviations from the fitted line are characterized by  $r^2$  values of 0.98 (ADF), 0.82 ( $G_1$ ), 0.95 ( $G_2$ ), and 0.97 ( $G_3$ ).

to higher frequencies when the Cp ring becomes more strongly bound to Zr (i.e., when the attachment of remaining ligands to Zr becomes looser). The best linear fit ( $\nu_m$ ) to the observed band positions is given by the equations  $\nu_m(\text{ADF}) = 1501 + 91q - 279d$ ,  $\nu_m(G_1) = 1561 + 65q - 326d$ ,  $\nu_m(G_2) = 1853 + 27q - 459d$ , and  $\nu_m(G_3) = 1751 + 23q - 415d$ , with  $q = Q(\text{Cp})$  in units of the elementary charge ( $e$ ) and  $d = d(\text{Zr}\text{--}\text{Cp})$  in Å. Predicted band positions based on these models are given in Table 2. The observed trends, which are independent of the choice of density functional and basis set, may be summarized as follows: (1) Cations and compounds with bridging ligands have higher frequencies than neutral compounds. Removing a ligand completely or partly, as with a bridge, decreases the electron density in

**Table 2.** Calculated Band Positions ( $\text{cm}^{-1}$ ) of the Cp Out-of-Plane Deformation On the Basis of the Calculated Mulliken Charge on the Cp Ring and the Distance Between Zr and the Center of the Cp Ring<sup>a</sup>

	compound	ADF	$G_1$	$G_2$	$G_3$
A	$\text{Cp}_2\text{ZrMe}_2$	803	804	804	802
	$\text{Cp}_2\text{ZrMeCl}$	810	811	811	811
	$\text{Cp}_2\text{ZrCl}_2$	817	817	816	818
B	$(\text{Cp}_2\text{ZrMe})_2(\mu\text{-O})$	795	794	794	795
	$[(\text{Cp}_2\text{ZrMe})_2(\mu\text{-Me})]^+$	819	819	819	818
	$\text{Cp}_2\text{ZrMe}(\mu\text{-Me})\text{BR}_3$	823	822	824	824
	$[\text{Cp}_2\text{Zr}(\mu\text{-Me})_2\text{AlMe}_2]^+$	831	830	831	830
	calibration $r^2$	0.98	0.95	0.98	0.96
validation $r^2$ <sup>b</sup>	0.91	0.80	0.89	0.78	

<sup>a</sup> See footnotes for Table 1 and text for details. <sup>b</sup> Validation  $r^2$  is based on a full leave-one-out cross-validation.

the Cp rings (i.e.,  $q$  increases) and leads to a shorter Cp–Zr distance (because all cations in this study are stabilized by bridging ligands, the effect of the total charge alone is not clear). (2) Compounds with methyl ligands have lower  $\nu$  values than compounds with chlorine ligands. Methyl is less electronegative than Cl, resulting in a more negative Cp ring. (3) Compounds with oxygen ligands tend to have low values of  $\nu$ . The two-coordinate oxygen is a good electron donor, resulting in a more negative Cp ring. Even in a three-coordinated bridging position between Zr and two Al atoms, as in the model structure  $\text{Cp}_2\text{ZrMe}(\mu_3\text{-O})\text{Al}_6\text{O}_5\text{Me}_7$ ,<sup>26</sup> oxygen forms a relatively strong bond to Zr, resulting in a fairly long Zr–Cp distance.

**Reactions with Aluminum Alkyls.** In the mixture of  $\text{Cp}_2\text{ZrCl}_2$  and  $\text{Cp}_2\text{ZrMe}_2$ , a slow exchange takes place, and  $\text{Cp}_2\text{ZrMeCl}$  is formed in good yield.<sup>15</sup> The reaction proceeds over several weeks. The original bands at 814 and  $803\text{ cm}^{-1}$  diminish, and a new strong band appears at  $809\text{ cm}^{-1}$ , characteristic of the product.

In agreement with earlier reports,  $\text{Cp}_2\text{ZrMeCl}$  was obtained in a moderate yield in the reaction of TMA with  $\text{Cp}_2\text{ZrCl}_2$ .<sup>4,5,27</sup> No IR band attributable to  $\text{Cp}_2\text{ZrMe}_2$  was observed. Further, no  $\text{Cp}_2\text{ZrMe}_2$  was detected when TMA was added to  $\text{Cp}_2\text{ZrMeCl}$  in a separate experiment; instead, the IR spectrum indicated the presence of a new species with the Cp out-of-plane deformation band at  $815\text{ cm}^{-1}$ . This result suggests the formation of a chlorine-bridged adduct,  $\text{Cp}_2\text{ZrMe}(\mu\text{-Cl})\text{AlMe}_3$ . The corresponding titanium complex is known.<sup>28,29</sup> The preference for a chlorine bridge over an electron-deficient methyl bridge is clearly demonstrated by the chlorine-bridged dimer of DMAC.<sup>30,31</sup>

No new compounds were observed in the mixture of  $\text{Cp}_2\text{ZrMe}_2$  and TMA; hence, the double methyl bridge of the TMA dimer is preferred to a single bridge between Zr and Al. The addition of DMAC to  $\text{Cp}_2\text{ZrMe}_2$  rapidly resulted in

- (26) (a) Zurek, E.; Ziegler, T. *Organometallics* **2002**, *21*, 83–92. (b) Zurek, E.; Ziegler, T. *Prog. Polym. Sci.* **2004**, *29*, 107–148.  
 (27) Cam, D.; Giannini, U. *Macromol. Chem.* **1992**, *193*, 1049–1055.  
 (28) Ott, K. C.; De Boer, E. J. M.; Grubbs, R. H. *Organometallics* **1984**, *3*, 223–230.  
 (29) Tritto, I.; Sacchi, M. C.; Li, S. *Macromol. Rapid Commun.* **1994**, *15*, 217–223.  
 (30) Brendhaugen, K.; Haaland, A.; Novak, P. D. *Acta Chem. Scand. A* **1974**, *28*, 45–47.  
 (31) Tarazona, A.; Koglin, E.; Buda, F.; Coussens, B. B.; Renkema, J.; van Heel, S.; Meier, R. J. *J. Phys. Chem. B* **1997**, *101*, 4370–4378.

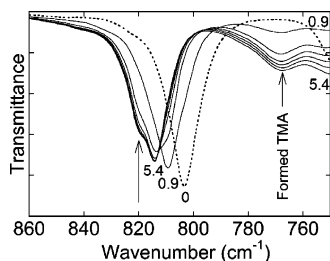


**Figure 4.** IR spectra acquired during the addition of DMAC to  $\text{Cp}_2\text{ZrMe}_2$  (at Al/Zr ratios of 0, 0.9, 1.8, 2.7, 3.6, 4.5, and 5.4; initial [Zr] = 0.05 M). The region of the out-of-plane Cp deformation is shown. After the first addition of DMAC (Al/Zr = 0.9), the band position is at  $809\text{ cm}^{-1}$  (because of  $\text{Cp}_2\text{ZrMeCl}$ ). At Al/Zr = 5.4, the main band is at  $814\text{ cm}^{-1}$  (because of  $\text{Cp}_2\text{ZrCl}_2$ ) with a shoulder at  $820\text{ cm}^{-1}$  (suggested to be the result of a chlorine-bridged adduct,  $\text{Cp}_2\text{ZrMe}(\mu\text{-Cl})\text{AlMe}_2\text{Cl}$ ). The spectra were recorded 3–4 min after the additions.

$\text{Cp}_2\text{ZrMeCl}$  and TMA as the first products (Al/Zr = 0.9). The addition of more DMAC (up to Al/Zr = 5.4) gave  $\text{Cp}_2\text{ZrCl}_2$  in high yield, identified by its IR band at  $814\text{ cm}^{-1}$ , and a new product, observed as a well-defined shoulder at  $820\text{ cm}^{-1}$ . The changes of the spectra in this region are shown in Figure 4. The system now contains several compounds that may form adducts,  $\text{Cp}_2\text{ZrMe}_2$ ,  $\text{Cp}_2\text{ZrMeCl}$ ,  $\text{Cp}_2\text{ZrCl}_2$ , DMAC, and TMA. No band was observed at  $820\text{ cm}^{-1}$  in any of the binary mixtures with TMA; hence, DMAC, rather than TMA, must be involved in the formation of the new species. In another experiment, no shoulder was observed at  $820\text{ cm}^{-1}$  when 5 equiv of DMAC was added to  $\text{Cp}_2\text{ZrCl}_2$ ; hence,  $\text{Cp}_2\text{ZrMeCl}$ , rather than  $\text{Cp}_2\text{ZrCl}_2$ , is the component involved. When the amount of DMAC was raised 1 order of magnitude until Al/Zr = 48, a weak shoulder was observed. Likely explanations in this case are the formation of  $\text{Cp}_2\text{ZrCl}(\mu\text{-Cl})\text{AlMe}_2\text{Cl}$  at a high Al/Zr ratio or a methylation of the zirconocene. The most likely cause of the shoulder at  $820\text{ cm}^{-1}$  in the  $\text{Cp}_2\text{ZrMe}_2$  and DMAC mixture is a chlorine-bridged adduct,  $\text{Cp}_2\text{ZrMe}(\mu\text{-Cl})\text{AlMe}_2\text{Cl}$ , formed by  $\text{Cp}_2\text{ZrMeCl}$  and DMAC. The corresponding titanium complex has been reported.<sup>28</sup>

Attempts to verify the presence of  $\text{Cp}_2\text{ZrMe}(\mu\text{-Cl})\text{AlMe}_3$  and  $\text{Cp}_2\text{ZrMe}(\mu\text{-Cl})\text{AlMe}_2\text{Cl}$  by proton NMR spectroscopy were not successful. When  $\text{Cp}_2\text{ZrCl}_2$  and a large excess of TMA were mixed to produce  $\text{Cp}_2\text{ZrMe}(\mu\text{-Cl})\text{AlMe}_3$ , the only new species identified were  $\text{Cp}_2\text{ZrMeCl}$  and DMAC. However, the methyl resonance of the zirconocene at 0.45 ppm was unusually wide, 25 Hz, which indicates the presence of a dynamic process. When  $\text{Cp}_2\text{ZrMe}_2$  and DMAC were mixed to produce  $\text{Cp}_2\text{ZrMe}(\mu\text{-Cl})\text{AlMe}_2\text{Cl}$ , several peaks were observed, but these could not be assigned unambiguously. Calculated frequencies support the interpretation in terms of chlorine-bridged adducts with predicted band positions of  $819 \pm 3\text{ cm}^{-1}$  for  $\text{Cp}_2\text{ZrMe}(\mu\text{-Cl})\text{AlMe}_3$  and  $820 \pm 2\text{ cm}^{-1}$  for  $\text{Cp}_2\text{ZrMe}(\mu\text{-Cl})\text{AlMe}_2\text{Cl}$  (based on the four DFT levels).

In summary, TMA is not able to dimethylate the zirconocene but causes the formation of  $\text{Cp}_2\text{ZrMeCl}$ . In systems containing chlorine, new products are formed, presumably bimetallic adducts bonded by a single chlorine bridge. None of the adducts were observed as the major component of their mixtures, consistent with the low calculated reaction energies for the formation of these adducts ( $1 \pm 2\text{ kcal/mol}$

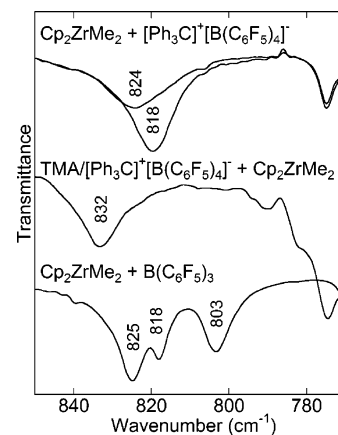


**Figure 5.** IR spectra of the reaction mixtures  $\text{Cp}_2\text{ZrMe}_2/\text{C}(\text{C}_6\text{H}_5)_3\text{B}(\text{C}_6\text{F}_5)_4$  (band position at  $818$  and  $824\text{ cm}^{-1}$  after 2 and 155 min, respectively),  $\text{Cp}_2\text{ZrMe}_2/\text{C}(\text{C}_6\text{H}_5)_3\text{B}(\text{C}_6\text{F}_5)_4/\text{TMA}$ , and  $\text{Cp}_2\text{ZrMe}_2/\text{B}(\text{C}_6\text{F}_5)_3$ . In all of the spectra, B/Zr = 1. The band at  $803\text{ cm}^{-1}$  in the lower spectrum is not a result of free  $\text{Cp}_2\text{ZrMe}_2$ . The DFT calculations suggest that this is caused by a vibrational mode in the  $\text{Cp}_2\text{ZrMe}(\mu\text{-Me})\text{B}(\text{C}_6\text{F}_5)_3$  complex involving B–( $\mu\text{-Me}$ ) stretch and  $\text{C}_6\text{F}_5$  in-plane and out-of-plane deformation.

for  $\text{Cp}_2\text{ZrMe}(\mu\text{-Cl})\text{AlMe}_3$  and  $0 \pm 5\text{ kcal/mol}$  for  $\text{Cp}_2\text{ZrMe}(\mu\text{-Cl})\text{AlMe}_2\text{Cl}$ ).

**Reactions with Boron Activators.** The literature contains extensive studies of the activation of metallocenes with boron-based activators.<sup>2</sup> In the present work, activation using the two well-characterized activators  $\text{B}(\text{C}_6\text{F}_5)_3$  and  $\text{C}(\text{C}_6\text{H}_5)_3\text{B}(\text{C}_6\text{F}_5)_4$  has been investigated with in situ IR spectroscopy. The purpose of studying them in this work was to obtain experimental frequencies for their reaction products with  $\text{Cp}_2\text{ZrMe}_2$ . These cocatalysts are known to produce the cations  $[(\text{Cp}_2\text{ZrMe})_2(\mu\text{-Me})]^+$  and  $[\text{Cp}_2\text{ZrMe}]^+$ . The latter will presumably not be present as a naked cation but will form tight and loose ion pairs with the counterions  $\text{MeB}(\text{C}_6\text{F}_5)_3^-$  and  $\text{B}(\text{C}_6\text{F}_5)_4^-$ , respectively. Solutions of the reagents were prepared and mixed directly in the in situ IR apparatus at room temperature. Samples were prepared for  $^1\text{H}$  NMR with the same procedures that were used for the IR experiments, and the main products and their order of appearance during the reaction were confirmed.

When  $\text{B}(\text{C}_6\text{F}_5)_3$  was added to  $\text{Cp}_2\text{ZrMe}_2$ , the first new band to appear in the  $800\text{ cm}^{-1}$  region was detected at  $818\text{ cm}^{-1}$  (B/Zr = 0.3). Further addition of  $\text{B}(\text{C}_6\text{F}_5)_3$  resulted in a new strong band at  $825\text{ cm}^{-1}$  (see Figure 5). Bands from free  $\text{B}(\text{C}_6\text{F}_5)_3$  were not observed until the B/Zr ratio exceeded unity, and at this point the reaction seemed to be complete as no further change was observed in the spectrum of the zirconocene. When the reactants were added in opposite order, starting with excess  $\text{B}(\text{C}_6\text{F}_5)_3$ , the band at  $818\text{ cm}^{-1}$  did not appear. In this system, the cation  $[(\text{Cp}_2\text{ZrMe})_2(\mu\text{-Me})]^+$  is known to be formed at low B/Zr ratios, while  $\text{Cp}_2\text{ZrMe}(\mu\text{-Me})\text{B}(\text{C}_6\text{F}_5)_3$  is formed at higher B/Zr ratios.<sup>4,32</sup> We therefore attribute the band at  $818\text{ cm}^{-1}$  to  $[(\text{Cp}_2\text{ZrMe})_2(\mu\text{-Me})]^+$  and the band at  $825\text{ cm}^{-1}$  to  $\text{Cp}_2\text{ZrMe}(\mu\text{-Me})\text{B}(\text{C}_6\text{F}_5)_3$ . The latter complex was also prepared outside the IR cell at low temperature as described by Yang et al.<sup>16</sup> The resulting

(32) Haselwander, T.; Beck, S.; Brintzinger, H. H. In *Ziegler Catalysts*; Fink, G., Mülhaupt, R., Brintzinger, H. H., Eds.; Springer: Berlin, 1995; pp 181–197.

IR spectrum essentially contained the same bands and an additional weak band with varying intensity and frequency between 813 and 818  $\text{cm}^{-1}$ . It is not clear whether the latter feature is a result of  $[(\text{Cp}_2\text{ZrMe})_2(\mu\text{-Me})]^+$  or another product.

The reactions of  $\text{Cp}_2\text{ZrMe}_2$  with  $\text{C}(\text{C}_6\text{H}_5)_3\text{B}(\text{C}_6\text{F}_5)_4$  were monitored in a similar experiment. A single band at 818  $\text{cm}^{-1}$  was clearly observed immediately after mixing but was gradually substituted with a band at 824  $\text{cm}^{-1}$  within a few hours. In this system, the binuclear cation  $[(\text{Cp}_2\text{ZrMe})_2(\mu\text{-Me})]^+$  appears to be kinetically preferred and is formed even with excess cocatalyst before it is slowly converted into  $[\text{Cp}_2\text{ZrMe}]^+$  (or rather weakly coordinating  $[\text{Cp}_2\text{ZrMe}]^+\cdots[\text{B}(\text{C}_6\text{F}_5)_4]^-$  ion pairs).<sup>14</sup> The band at 818  $\text{cm}^{-1}$  is therefore attributed to the binuclear cation and the band at 824  $\text{cm}^{-1}$  to  $[\text{Cp}_2\text{ZrMe}]^+$ . The addition of TMA to this mixture immediately resulted in a new band at 832  $\text{cm}^{-1}$ . The same band was also obtained when  $\text{Cp}_2\text{ZrMe}_2$  was added to a mixture of TMA and boron activator. We attribute this band to the binuclear cation  $[\text{Cp}_2\text{Zr}(\mu\text{-Me})_2\text{AlMe}_2]^+$ . In Figure 5, the 800  $\text{cm}^{-1}$  region of the IR spectra of three reaction mixtures in these systems is shown.

The IR data obtained in the boron-based systems show that important intermediates can be identified by IR as well as by NMR spectroscopy. Also, the DFT calculations support the assignment of the experimentally observed IR bands (see Table 1 and Figure 3). Using the linear fit between the calculated and observed band positions, the band for the binuclear cation  $[(\text{Cp}_2\text{ZrMe})_2(\mu\text{-Me})]^+$  is predicted to be in the 815–820  $\text{cm}^{-1}$  range at the four computational levels (see the Overview). The band for the methyl-bridged complex,  $\text{Cp}_2\text{ZrMe}(\mu\text{-Me})\text{B}(\text{C}_6\text{F}_5)_3$ , is correspondingly predicted to be in the 824–829  $\text{cm}^{-1}$  range. Somewhat surprisingly, the band position of the naked cation  $[\text{Cp}_2\text{ZrMe}]^+$  is predicted to be in the 825–830  $\text{cm}^{-1}$  range, in good agreement with the experimental value. On the basis of its low electron density on the Cp rings and small Zr–Cp distance, one might have expected a band position at higher frequency. Finally, the position of the band of the cation  $[\text{Cp}_2\text{Zr}(\mu\text{-Me})_2\text{AlMe}_2]^+$  is predicted to be in the 827–833  $\text{cm}^{-1}$  range. As can be seen in Table 1, these are all in agreement with experimental frequencies.

**Reactions with MAO.** In this section, we report the results of in situ IR studies of the reactions of  $\text{Cp}_2\text{ZrCl}_2$  and  $\text{Cp}_2\text{ZrMe}_2$  with MAO at low Al/Zr ratios. New bands were immediately observed at 820 and 822  $\text{cm}^{-1}$  for  $\text{Cp}_2\text{ZrCl}_2$  and  $\text{Cp}_2\text{ZrMe}_2$ , respectively, showing that at least one new product is formed. When  $\text{Cp}_2\text{ZrCl}_2$  was used, there was a substantial decrease in the intensity of the band attributed to the bridging methyl groups in MAO at 1257  $\text{cm}^{-1}$ . As shown in Figure 6, the changes are similar to those produced by addition of DMAC to MAO, where MAO is chlorinated by DMAC. The top frame shows a comparison between MAO and the recovered MAO after reaction with DMAC. The bottom frame shows MAO before and after the addition of  $\text{Cp}_2\text{ZrCl}_2$ . We have previously shown that only the bridging methyls in MAO are exchangeable with the chlorine of DMAC, and even in the presence of TMA, the chlorinated

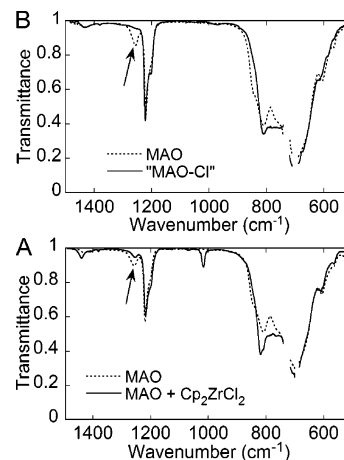


**Figure 6.** B: IR spectra of normal and chlorinated MAO (MAO after reaction with DMAC and subsequent workup<sup>7</sup>). A: Effect on the spectrum of MAO by addition of  $\text{Cp}_2\text{ZrCl}_2$  (Al/Zr = 10, [Zr] = 0.1 M).

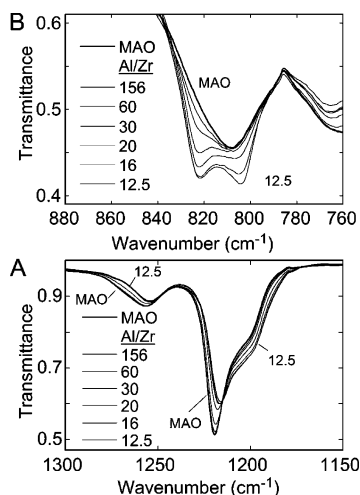


**Figure 7.** IR spectra of mixtures of  $\text{Cp}_2\text{ZrMe}_2$  and MAO in toluene at progressively higher concentrations of zirconocene. A: Symmetrical deformation of methyl on Al. B: Cp out-of-plane deformation superimposed on MAO bands (initial [Al] = 0.5 M, final [Al] = 0.33 M, [Zr] = 0.027 M). The solvent component of the spectra has been removed. The spectra have been slightly scaled to compensate for the random variations in intensity caused by phase separation.

MAO was unable to activate  $(\text{Me}_5\text{C}_5)_2\text{ZrCl}_2$ .<sup>7</sup> Clearly, the methyl bridges in MAO are essential to the activation of the catalyst. In the mixture of MAO and  $\text{Cp}_2\text{ZrCl}_2$ , it was not possible spectroscopically to determine if the chlorines form Zr–Cl–Al links or go into Al–Cl–Al environments with methyl or oxygen as the bridging unit between MAO and the zirconocene. DFT calculations suggest that the combination of Al–Cl–Al and Zr–Me–Al is preferred over Al–Me–Al and Zr–Cl–Al by about 5 kcal/mol, but kinetic effects may play a role.

The subsequent studies were performed with  $\text{Cp}_2\text{ZrMe}_2$  to exclude any ambiguity concerning the chlorine or methyl groups. In Figure 7, spectral changes upon the addition of  $\text{Cp}_2\text{ZrMe}_2$  to MAO are shown. The series of IR spectra was recorded at progressively higher concentrations of zirconocene. Unfortunately, in concentrated samples, a phase separation takes place, and the random distribution of the two phases in the IR cell influences the intensity of the spectrum. A quantitative analysis is therefore not possible,

but a careful scaling of the spectra allows trends to be observed on the basis of the shape of the band envelope. The scaling procedure is described in the Experimental Section.

Distinct changes indicative of a reaction are observed in several regions of the IR spectrum when  $\text{Cp}_2\text{ZrMe}_2$  and MAO are mixed. The bands in the 1150–1300  $\text{cm}^{-1}$  region, shown in Figure 7A, are caused by the symmetric deformations of methyls on MAO. The band at 1257  $\text{cm}^{-1}$  is assigned to the bridging methyls, while the group of bands below 1240  $\text{cm}^{-1}$  represents different terminal methyls.<sup>7</sup> The Cp out-of-plane deformation bands around 800  $\text{cm}^{-1}$  (Figure 7B) are superimposed on the strong broad Al–O stretching/methyl rock band of MAO centered at 808  $\text{cm}^{-1}$ .<sup>33</sup> At the highest Al/Zr ratios, the only new band in this region is observed at 822  $\text{cm}^{-1}$ . The absence of a sharp band at 803  $\text{cm}^{-1}$  indicates that all or most of the zirconocene has reacted. This band was not observed until further addition of zirconocene brought the Al/Zr ratio below 30. The bands attributed to the symmetric methyl deformations of MAO at 1200–1270  $\text{cm}^{-1}$  changed in shape with the addition of  $\text{Cp}_2\text{ZrMe}_2$  until an Al/Zr ratio of 15–20 was reached. Further additions had no effect on these bands, consistent with the observation of free  $\text{Cp}_2\text{ZrMe}_2$ . Changes were also found in the region of C–H stretching, but the interpretation is complicated by band overlap. Except for the fluctuations caused by the phase separation, the spectrum was stable for several hours. From the described behavior, there appears to be an equivalence point at Al/Zr = 15–20. At higher Al/Zr ratios, no free  $\text{Cp}_2\text{ZrMe}_2$  is observed while MAO is changing. At lower Al/Zr ratios,  $\text{Cp}_2\text{ZrMe}_2$  is observed, but no changes are seen in the MAO bands.

Upon addition of excess TMA to a mixture of MAO and  $\text{Cp}_2\text{ZrMe}_2$  (Al<sub>TMA</sub>/Zr = 11), the band at 822  $\text{cm}^{-1}$  disappeared, and a new band was observed at 816  $\text{cm}^{-1}$ . In contrast to the boron-based system with  $\text{C}(\text{C}_6\text{H}_5)_3\text{B}(\text{C}_6\text{F}_5)_4$ , no band for  $[\text{Cp}_2\text{Zr}(\mu\text{-Me})_2\text{AlMe}_2]^+$  was detected at 832  $\text{cm}^{-1}$ . Spectroscopic evidence for this cation has been reported but only at high Al/Zr ratios.<sup>3</sup> The source of the new band at 816  $\text{cm}^{-1}$  has not been identified.

**Monomer Insertion.** To study the changes in the IR spectrum on monomer insertion, 1-hexene was added to solutions of activated catalyst. When 1-hexene was added to the  $\text{Cp}_2\text{ZrMe}_2$ /MAO system, the IR band at 822  $\text{cm}^{-1}$  disappeared, and a broad band appeared around 815  $\text{cm}^{-1}$ . This was followed by a decrease in the bands attributed to the olefinic group of 1-hexene. The appearance of a new band at 886  $\text{cm}^{-1}$  characteristic of the vinylidene end groups of poly-1-hexene verifies catalytic activity. When MAO was added to a solution of 1-hexene and  $\text{Cp}_2\text{ZrMe}_2$ , the band at 822  $\text{cm}^{-1}$  did not appear at all, and catalytic activity was observed. The monomer was also added to a solution of  $\text{Cp}_2\text{ZrMe}_2(\mu\text{-Me})\text{B}(\text{C}_6\text{F}_5)_3$ .<sup>34</sup> The band at 825  $\text{cm}^{-1}$ , attributed to

this complex, immediately disappeared followed by 1-hexene consumption. Catalytic activity at a low Al/Zr ratio with a chlorine-free system and a TMA-depleted MAO has also been reported by Pedetour et al.<sup>5</sup>

## Discussion

A substantial problem in the use of metallocene-based catalysts is the large excess of MAO required to obtain high polymerization activity. Although some MAO is simply consumed in the reaction with impurities and passivated by chlorination, a solid understanding of the need for such a great excess is not at hand. One possible explanation is that the activation is carried out by a minority species holding extraordinary properties, such as very high Lewis acidity or charge capacity. This would suggest a large potential for improvement if the rare MAO species could be identified and its formation optimized. On the other hand, if the large amount of MAO is needed to force an equilibrium reaction in the desired direction, the answer to the challenge is different.

The observation of a new IR band at 822  $\text{cm}^{-1}$  in the MAO/ $\text{Cp}_2\text{ZrMe}_2$  system, the accompanying changes in the bands around 1200  $\text{cm}^{-1}$ , and the absence of the  $\text{Cp}_2\text{ZrMe}_2$  band at 803  $\text{cm}^{-1}$  indicate that an extensive reaction is taking place, even at low Al/Zr ratios. When the Al/Zr ratio is brought below 15–20 by the addition of more  $\text{Cp}_2\text{ZrMe}_2$ , the changes in the MAO bands cease, and the  $\text{Cp}_2\text{ZrMe}_2$  bands appear, suggesting a MAO unit of 15–20 aluminum atoms that is able to react with a single zirconocene molecule. It is interesting that this number corresponds to the average size of MAO molecules as determined by cryoscopy.<sup>35</sup> An association of  $\text{Cp}_2\text{ZrMe}_2$  and MAO at a low Al/Zr ratio was also detected by Babushkin et al., but their results indicate that a slightly higher Al/Zr ratio is required to consume all of the  $\text{Cp}_2\text{ZrMe}_2$ .<sup>3</sup>

Bonding between MAO and the metallocene may occur through a methyl group or oxygen.<sup>3,26,36</sup> In the mixture of  $\text{Cp}_2\text{ZrMe}_2$  and  $\text{B}(\text{C}_6\text{F}_5)_3$ , a methyl-bridged compound is formed. Similar methyl-bridged adducts are likely to form with MAO as well. On the basis of <sup>13</sup>C NMR spectroscopy, a reversible methyl-bridged adduct has been suggested by Babushkin et al.<sup>3</sup> Zr–O bonding has been verified for  $\text{Cp}_2\text{ZrMe}_2$  and a *tert*-butyl aluminoxane with a strained structure and no alkyl bridges.<sup>37</sup> The *tert*-butyl aluminoxane cage reacts in a similar manner with TMA, forming bridging methyls while strain is released.<sup>38</sup> Since a significant amount of TMA is always present in commercial MAO solutions, we argue that the strained Al–O bonds are already opened, occupied by TMA, and no longer available for the metallocene. Instead, there are bridging methyl groups with reactive electron-deficient bonds. This is consistent with the reported high cocatalytic activity of the *tert*-butyl aluminoxane cage after reaction with TMA.<sup>38</sup>

(33) The calculations predict that deuteration of the Cp ligands will lower the Cp out-of-plane deformation to around 600  $\text{cm}^{-1}$ , but there will still be an overlap with a MAO band of medium intensity at 605  $\text{cm}^{-1}$  (see Figure 6).

(34) Solution of the complex prepared at low temperature.

(35) Sinn, H. *Macromol. Symp.* **1995**, 97, 27–52.

(36) Kaminsky, W.; Steiger, R. *Polyhedron* **1988**, 7, 2375–2381.

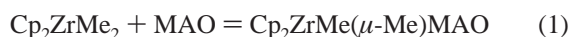
(37) Harlan, C. J.; Bott, S. G.; Barron, A. R. *J. Am. Chem. Soc.* **1995**, 117, 6465–6474.

(38) Watanabe, M.; McMahon, C. N.; Harlan, C. J.; Barron, A. R. *Organometallics* **2001**, 20, 460–467.

We have calculated (at the  $G_1$  level) the IR spectrum of the two candidates, oxo-bridged  $\text{Cp}_2\text{ZrMe}(\mu_3\text{-O})\text{Al}_6\text{O}_5\text{Me}_7$  and methyl-bridged  $\text{Cp}_2\text{ZrMe}(\mu\text{-Me})\text{Al}_8\text{O}_6\text{Me}_{12}$ , for the adduct responsible for the observed band at  $822\text{ cm}^{-1}$ .<sup>39</sup> The former would be the result of a reaction between  $\text{Cp}_2\text{ZrMe}_2$  and a  $\text{Me}_6\text{Al}_6\text{O}_6$  MAO cage with only terminal methyl groups and  $\text{Me}/\text{Al} = 1.0$ . The latter would be the result of a reaction between  $\text{Cp}_2\text{ZrMe}_2$  and a more realistic MAO structure,  $\text{Me}_{12}\text{Al}_8\text{O}_6$ , with methyl bridges and  $\text{Me}/\text{Al} = 1.5$ . In both cases, the Cp out-of-plane deformations are coupled to other vibrations of the adduct. In the calculations, several bands are present in the  $760\text{--}840\text{ cm}^{-1}$  region, both in the MAO cage itself and in the two anticipated MAO/zirconocene adducts. For example, the methyl-bridged adduct has an almost linear methyl bridge between Zr and Al; this bridge has deformation modes coupled to Cp out-of-plane vibrations that are candidates for the observed band at  $822\text{ cm}^{-1}$ . Furthermore, since the complexity of the real MAO solution is not fully expressed by a single structure, the experimental and calculated spectra are not easily compared in this case. It is therefore not possible to determine if the new band at  $822\text{ cm}^{-1}$  is caused by a shift of the Cp out-of-plane vibrational mode or by changes in other characteristic modes upon adduct formation.

The question of whether the complex is linked by oxygen or methyl is not resolved by the experiments. However, we will argue that a methyl-bridged MAO/zirconocene adduct is more likely than an oxo-bridged one. First, the presence of methyl bridges in MAO is evident through the IR band at  $1257\text{ cm}^{-1}$ . This is also clearly verified in the calculated spectrum of MAO. Second, the formation of a Zr–O bond requires that a rather strong Al–O bond be broken (assuming only three-coordinate oxygen and the absence of highly strained Al–O bonds). Presumably, the methyl bridge in MAO is the most reactive feature and will easily open up to form the new connection. The following discussion of a possible activation mechanism is, therefore, based on the methyl-bridged adduct.<sup>40</sup>

The rapid and extensive reaction of  $\text{Cp}_2\text{ZrMe}_2$  with MAO at a low Al/Zr ratio has an implication on the discussion of the activation process. Consider a simple two-step activation process starting with eq 1 followed by eq 2 and that the product of eq 2 is active or is activated by the monomer.



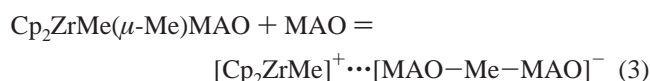
Since MAO quickly consumes the free  $\text{Cp}_2\text{ZrMe}_2$ , the large excess of MAO is not necessary to drive eq 1 to the product side. The production of a free cation, eq 2, seems to be the limiting step. How can excess MAO help in this case?

(39) Although the  $[(\text{Cp}_2\text{ZrMe})_2(\mu\text{-Me})]^+$  cation has a band in roughly the right position, NMR results show that it is not generated in a high yield at this low Al/Zr ratio (ref 4).

(40) A related scheme was sketched by Kaminsky and Steiger (ref 36) using an oxygen-bridged adduct. However, the linear representation used for MAO does not reflect the real availability of unsaturated oxygen.

The prevailing explanation in the literature is that MAO has sites with different Lewis acidities, and only the most acidic sites are able to weaken the methyl–zirconium bond sufficiently to form ion pairs. We would like to draw attention to an alternative explanation complementary to the action of superacidic rare species.

The need for stabilization of the cation, by either the olefin, TMA, or another weak donor, has been extensively discussed in the literature.<sup>2</sup> The need for additional stabilization of the anion has received less attention. Marks et al.,<sup>2</sup> in their work on noncoordinating boron activators, have demonstrated the importance of both steric hindrance and charge dissipation at the anion to promote activation of the metallocene. A single MAO cage may not provide adequate charge dissipation, resulting in an overly strong interaction with the metallocene. With excess MAO, additional MAO cages will compete with the zirconocene cation and may form dual cage anions,  $[\text{MAO-Me-MAO}]^-$ , that provide better shielding of the negative charge. The second equilibrium, now with MAO on the reactant side, becomes



Calculations, using a  $\text{Me}_{12}\text{Al}_8\text{O}_6$  cage model with methyl bridges, show that the energy expense of forming a separated ion pair is lowered by as much as 20 kcal/mol with eq 3 compared to that of eq 2. A similar result was obtained by Ustynyuk and Fushman with  $\text{Al}(\text{C}_6\text{F}_5)_3$ .<sup>41</sup> This contribution to ion pair separation is of the same order as the effect of monomer coordination. The activation sequence is depicted in Figure 8. The MAO model can be described as a hexagonal cage (side view) opened at opposite sides to accommodate two  $\text{AlMe}_3$  units.

For simplicity, we have not considered the formation of  $[\text{Cp}_2\text{Zr}(\mu\text{-Me})_2\text{AlMe}_2]^+$  and  $[(\text{Cp}_2\text{ZrMe})_2(\mu\text{-Me})]^+$  in this model. It is easily expanded to include these bimetallic cations, but this part will not deviate from previous works. The failure to observe  $[\text{Cp}_2\text{Zr}(\mu\text{-Me})_2\text{AlMe}_2]^+$  when MAO and TMA were added may be a consequence of the low Al/Zr ratio, or the band may be masked by changes in the underlying shoulder at  $840\text{ cm}^{-1}$  in the MAO spectrum.

## Conclusions

Changes in the position of the out-of-plane vibration of the hydrogen atoms on the Cp ring are correlated with changes in the bonding environment around Zr in various zirconocenes and zirconocene complexes. On the basis of DFT calculations, which reproduce the experimentally observed trends, it is found that the position of this band increases with increasing electron density on the Cp ring and decreases with increasing distance from Zr to the Cp ring. In binary mixtures of  $\text{Cp}_2\text{ZrMe}_2$ ,  $\text{Cp}_2\text{ZrCl}_2$ , DMAC, and TMA, new products were observed, except for TMA/ $\text{Cp}_2\text{-}$

(41) Ustynyuk, L. Yu.; Fushman, E. A. *Russ. J. Phys. Chem.* **2004**, *78*, 936–942.



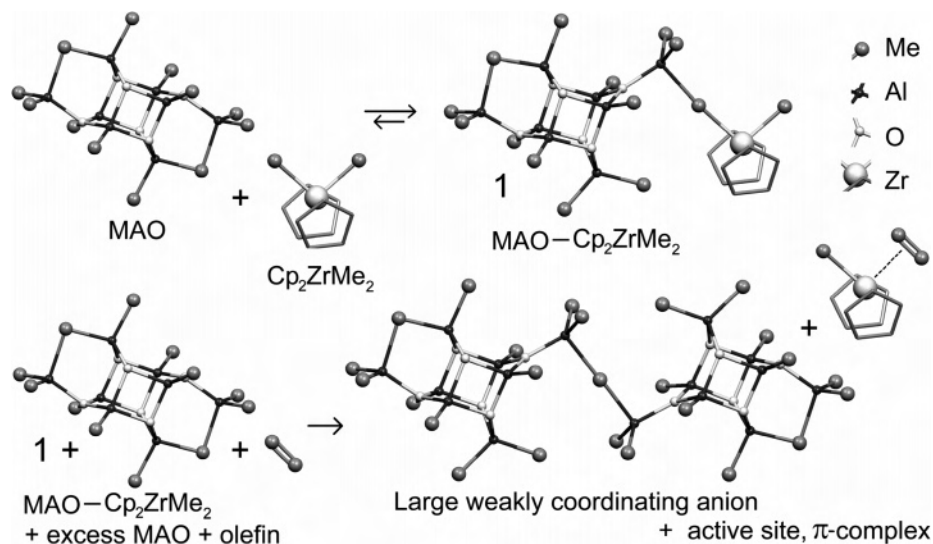


**Figure 8.** Ball and stick model of the suggested mechanism for zirconocene activation with MAO. A relatively small MAO cage model,  $\text{Me}_{10}(\mu\text{-Me})_2\text{-Al}_8\text{O}_6$ , is used and viewed slightly tilted off its  $C_2$  axis. Hydrogen atoms are not shown.

$\text{ZrMe}_2$  (and TMA/DMAC). The new products were  $\text{Cp}_2\text{-ZrMeCl}$  and bridged hetero-bimetallic complexes. In the mixture of MAO and  $\text{Cp}_2\text{ZrMe}_2$ , a new stable complex, most likely involving a methyl bridge between Zr and Al, is observed with an IR band at  $822\text{ cm}^{-1}$ . It is rapidly formed at low Al/Zr ratios and is proposed to be a precursor to the active catalyst. A mechanism is suggested for the activation of the metallocenes with MAO that is consistent with the need for a large excess of MAO. A key feature of this mechanism is formation of MAO cage dimers or oligomers

that tend to spread out the charge of the anion and facilitate formation of the active cation.

**Acknowledgment.** Financial support from the Norwegian Research Council (NFR) under the Polymer Science Program and Borealis is gratefully acknowledged. We are grateful to Albemarle Corporation for the donation of the sample of boron activator  $(\text{C}(\text{C}_6\text{H}_5)_3\text{B}(\text{C}_6\text{F}_5)_4)$ .

IC0482638